Thermodynamic Study on a Chiral Glass Former, 4-(1-Methylheptyloxy)-4′-cyanobiphenyl§

Kazuya Saito,*,†,‖ Maria Massalska-Arodz,†,‡ Satoaki Ikeuchi,† Masashi Maekawa,† Jacek Sciesinski,‡ Ewa Sciesinska,‡ Jacek Mayer,†,‡ Tadeusz Wasiutynski,†,‡ and Michio Sorai†

Research Center for Molecular Thermodynamics, Graduate School of Science, Osaka University, Toyonaka, Osaka 560-0043, Japan, and The Henryk Niewodniczanski Institute of Nuclear Physics, Polish Academy of Sciences, Radzikowskiego 152, 31-342 Kraków, Poland

Received: January 15, 2004; In Final Form: March 2, 2004

The heat capacities were measured by adiabatic calorimetry down to 6 K on both the right-handed isomer and a racemic mixture of 4-(1-methylheptyloxy)-4′-cyanobiphenyl. A thermodynamic relationship between two crystalline phases has been established and inversion between the stable and the metastable crystals has been found for the isomer. The contradiction between a previous calorimetric study and the results of inelastic neutron scattering and infrared spectroscopy has been resolved. No crystallization was detected for the racemic mixture. The behavior around the glass transition has been analyzed.

Introduction

For most organic substances a liquid-quenched glass (LQG) is realized on fast cooling (e.g., 10 K min^{-1} or greater). For polymers vitrification occurs at relatively high temperatures even when a sample is cooled slowly (ca. 1 K min^{-1}). Such type of behavior was observed also for low weight molecular organic materials such as alcohols. This class of substances was called as glass formers. It has been widely assumed that there are some universal properties on approaching glass transition temperature T_g. The clarification of such universal properties is extensively studied as one of the most challenging problems in soft-matter physics.[1−5]

Glass is nowadays understood in a broader sense. It is a nonequilibrium state with some frozen-in disorder.[6] The glass transition takes place at the temperature where the motional correlation time of some degrees of freedom exceeds the time scale of daily life (ca. 10^3 s). That is, the dynamical disorder above T_g is frozen-in below T_g. Plastic crystals,[7,8] liquid crystals,[9,10] and some crystals with structural disorder[11−14] show glass transitions. It is still an open problem to what extent the universal properties observed in LQG's are common to these glasses in this broader sense.[15]

The title compound is a glass former giving a LQG and has been studied with several experimental methods.[16−19] At room temperature the compound is a liquid. Despite the elongated shape of the 8*OCB molecules no liquid crystalline phase has been detected although 8OCB, which has a linear chain, is mesogenic.[20] In the dielectric spectroscopy studies[16] it was found that on cooling a chiral isomer (c-8*OCB) at a rate of 0.2 K min^{-1} only a LQG was formed. On heating the sample, first a softening of the LQG around 220 K, then a crystallization starting at 250 K and a melting at 285 K were observed. Adiabatic calorimetry measurements down to 100 K have revealed several new features of the polymorphism.[17] At least two crystalline phases, C_1 and C_2, have been identified. On cooling the liquid to 200 K at a rate of 0.12 K min^{-1} a crystallization to the C_1 phase has been detected below 270 K either for the whole sample or for its part. On subsequent heating, part of the LQG showed the softening at 219 K and then crystallization occurred around 260 K. Melting of the C_1 phase was observed at 288 K. The second crystalline phase, i.e., the C_2 phase, was formed just after melting of the C_1 phase and melted at 294 K. In one experimental run a direct crystallization of the supercooled liquid into the C_2 phase was observed at 264 K. Despite some attempts no direct transformation of the C_1 to the C_2 phase has been detected. The heat capacity of the C_2 phase that is stable around room temperature is larger than that of the C_1 phase. Infrared absorption spectra[17,18] for these three solid forms obtained at 100 K according to the cooling/heating treatment adopted in calorimetry are reproduced in Figure 1. The spectrum of the C_1 phase is well resolved as is often the case for ordered molecular crystals. An interesting point is that the spectra of the LQG and the C_2 phase show certain similarities typical for amorphous phases especially at low wavenumber below 100 cm^{-1}. Optical texture observation done by polarizing microscopy[17] indicated that crystallites of the C_1 phase are better developed and of higher anisotropy than that of the C_2 phase. The spectra of the vibrational density of states $G(\nu)$ obtained by incoherent inelastic neutron scattering[19] at 20 K in Figure 2 also provide evidence that the C_1 phase is well-ordered in comparison to the C_2 phase. Below 50 cm^{-1}, the C_2 phase with the highest density of states seems to be even less ordered than the LQG. Change of the infrared spectra in the vicinity of room temperature as well as the maximum value of single interferogram vs time and temperature has shown clearly two-step melting in accordance with the calorimetric results.

These findings are peculiar in some respects. That is, the C_2 phase, which seems to be the most stable at room temperature, shows the broad IR spectra at low temperatures and large vibrational density of states at low energies, both of which are typical for disordered solids. The aims of this paper are to clarify this apparent inconsistency on the basis of precise calorimetry in an expanded temperature range and to give some information on the glass transition of the LQG. In this paper, the results of adiabatic calorimetry on both c-8*OCB and a racemic mixture of 8*OCB (r-8*OCB) are described in detail. The behavior around the glass transition is also discussed.

* Corresponding author. E-mail:kazuya@chem.tsukuba.ac.jp.

§ Contribution No. 84 from the Research Center for Molecular Thermodynamics.

† Osaka University.

‡ Polish Academy of Sciences.

‖ Present address: Department of Chemistry, Graduate School of Pure and Applied Sciences, University of Tsukuba, Tsukuba, Ibaraki 305-8571, Japan.

10.1021/jp049777v CCC: $27.50
Published on Web 04/13/2004

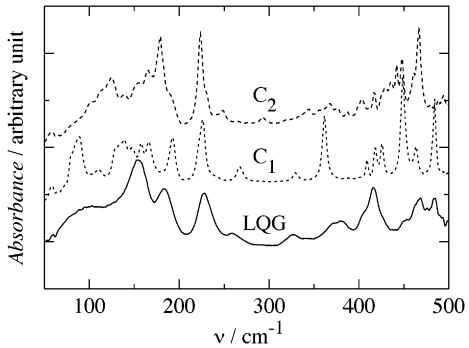

Figure 1. Infrared spectra for the LQG and C_1 and C_2 phases of c-8*OCB in the wavenumber range between 50 and 500 cm^{-1} at 100 K.[17] The spectra are drawn shifting vertically for ease of viewing.

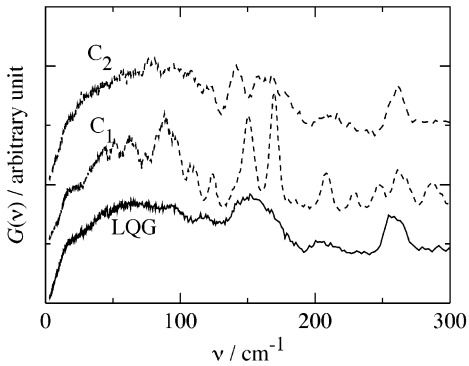

Figure 2. Vibrational density of states, $G(\nu)$, of the LQG and C_1 and C_2 phases of c-8*OCB obtained by the inelastic neutron scattering at 20 K. The spectra are shifted vertically for clarity.

Experimental Section

8*OCB was synthesized at the Institute of Chemistry, Military University of Technology, Warsaw. The purity of the sample of c-8*OCB was determined as 99.95 mol % by cryoscopy as described later. The chemical analysis yielded the following results (calculated values): C 81.96% (82.04%), H 8.22% (8.20%), N 4.54% (4.56%) for c-8*OCB and C 81.69%, H 7.88%, N 4.62% for r-8*OCB. It is clear that in the present experiments the c-8*OCB is of a higher quality than r-8*OCB.

The specimens were degassed before loading into a gold-plated copper calorimeter vessel, which was sealed after introducing a small amount of helium gas (10^5 Pa at room temperature) for thermal exchange inside the vessel. The mass of the substance loaded was 2.4129 g (7.8486 mmol) in the case of c-8*OCB and 2.2332 g (7.2641 mmol) for r-8*OCB, after buoyancy correction. The samples contributed more than 30% of the total heat capacity including that of the vessel and the helium gas.

The measurements were made by a laboratory-made adiabatic calorimeter at Osaka University up to 300 K. The working thermometers mounted on the calorimeter vessel were platinum (MINCO, S1055) and germanium (Lake-Shore, GR-200B-500) resistance thermometers for use above and below 13.8 K, respectively. Their temperature scales are based upon the ITS-90. The details of design, operation, and performance of the adiabatic calorimeter are described elsewhere.[21]

Results and Discussion

A. General Phase Behavior. A general phase behavior of c-8*OCB coincided with the previous results by Polish authors in ref 17: Cooling (-4.2 K min^{-1} around 280 K) of the liquid from room temperature results in the formation of the LQG around 220 K. The LQG is transformed to a thermodynamically metastable supercooled liquid above the glass transition around 220 K on heating. Further heating induces a crystallization of this supercooled liquid around 236 K to the C_1 phase, which melts around 288 K. The resultant liquid is recrystallized again to the C_2 phase, which melts around 294 K.

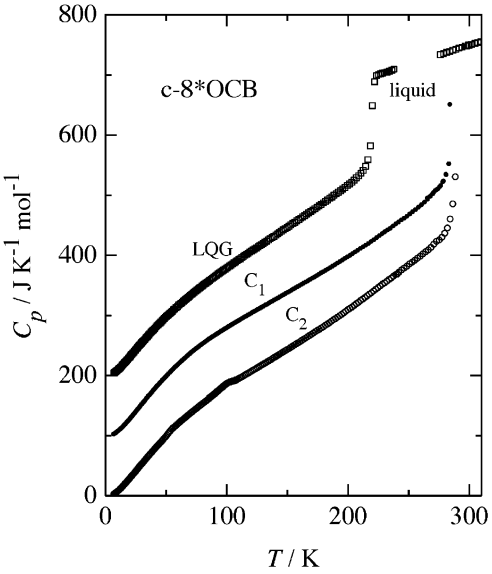

Figure 3. Heat capacities of the liquid and solid forms of c-8*OCB: square, LQG and liquid; filled circle, C_1 phase; open circle, C_2 phase. The ordinate is for the C_2 phase. The other data are successively shifted upward by 100 J K^{-1} mol^{-1}.

The heat capacities of three solid forms (C_1 and C_2 phases and LQG) and supercooled liquid were measured after carefully cooling the sample in the appropriate states down to the desired temperatures. Typical results are shown in Figure 3. The lack of C_p data for the liquid between 240 and 275 K is due to the spontaneous crystallization of the supercooled liquid into the C_1 phase observed on heating the sample after rapid cooling to liquid-nitrogen temperature.

For r-8*OCB, the LQG was the only solid form realized in this study. Indeed, to realize possible crystallization, we tried to keep the sample heated from the LQG state for 100 h under an adiabatic condition at 240 K, the temperature around which c-8*OCB undergoes crystallization. However, no symptom of crystallization was detected. The absence of the tendency to form any crystals for racemic mixtures is also observed in a typical glass former propylene glycol,[22] and implies one or both of the following: no stable crystal exists for this racemic mixture and the crystallization is kinetically inhibited more severely in r-8*OCB than the c-8*OCB. The heat capacities of r-8*OCB are compared with those of c-8*OCB in Figure 4. The temperature dependence of the heat capacity of r-8*OCB is closely similar to that of c-8*OCB, including the location of the glass transition.

B. Fusion of c-8*OCB and Cryoscopy. The so-called fractional-melting method was applied for the fusion of the C_2 phase. The method is based on the melting point depression: Since the amount of the impurity sealed in the calorimetric vessel is constant, the fraction melted in the vessel is inversely proportional to the concentration of the resultant solution of unkown impurities as far as the impurity is assumed to be liquid soluble but solid insoluble. The result is shown in Figure 5. The temperature of fusion of the C_2 phase of the calorimetric sample and that of the ideally pure compound are determined as 294.07 and 294.29 K, respectively. From the enthalpy of

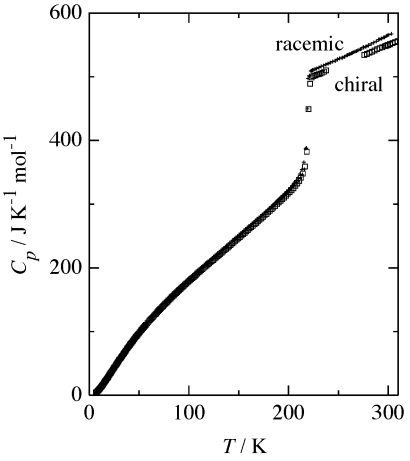

Figure 4. Comparison of the heat capacities of c-8*OCB and r-8*OCB: square, c-8*OCB; cross, r-8*OCB.

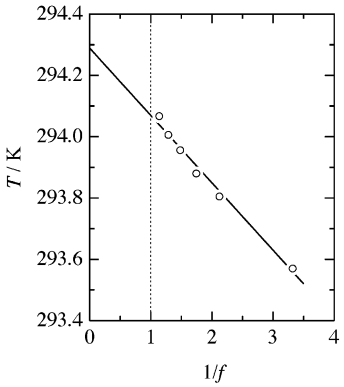

Figure 5. Equilibrium temperatures as a function of the inverse of the fraction melted (f) upon the fusion of the C_2 phase.

fusion (17.07 kJ mol^{-1}) and the slope of the straight line in Figure 5, the purity of the calorimetric sample was determined as 99.95 mol %. The high purity thus determined is consistent with the result of chemical analysis. The entropy of fusion derived from the enthalpy gain is 58.0 J K^{-1} mol^{-1}.

It seemed impossible to apply the fractional melting method to the fusion of the C_1 phase because the recrystallization to the stable C_2 phase was expected. Fortunately, the equilibrium between the C_1 phase and the supercooled liquid was followed for several hours under the adiabatic condition. The fraction melted was also successfully estimated from the amount of heat input based on the enthalpy of fusion (19.51 kJ mol^{-1}). Since the purity of the calorimetric sample is known from the experiment on the C_2 phase, the temperatures of fusion of the C_1 phase of the calorimetric sample and the ideally pure compound are deduced as 287.37 and 287.55 K, respectively. The enthalpy of fusion corresponds to the entropy of fusion of 67.9 J K^{-1} mol^{-1}.

Thermodynamic quantities upon fusion are summarized in Table 1. Also shown are the previous results reported by Polish authors in ref 17. Although the absolute values are a little bit different between the present and the previous report,[17] a similar tendency has been found.

C. Stable Phase Sequence of c-8*OCB. Primary data of the heat capacity were smoothed out by using a least-squares fit procedure in each temperature region appropriately divided. Standard thermodynamic quantities such as enthalpy function, entropy increment, and the Gibbs energy function were obtained from appropriate integration of the resulting fits. In the calculation, the C_1 phase was assumed to obey the third law of thermodynamics, as there is no anomaly in the temperature dependence of heat capacity down to the lowest temperature (6 K).

TABLE 1: Summary of Thermal Anomalies of c-8*OCB

phase	thermodynamic quantites
C_1 phase	
fusion	T_{fus} = 287.55 K,[a] 287.37 K[b] (287.8 K)[c]
	$\Delta_{fus}H$ = 19.51 kJ mol^{-1} (20.8 kJ mol^{-1})[c]
	$\Delta_{fus}S$ = 67.9 J K^{-1} mol^{-1} (72.3 J K^{-1} mol^{-1})[c]
trasition to C_2 phase[d]	T_x = 244.39 K
	$\Delta_{trs}H$ = 1.9 kJ mol^{-1}
	$\Delta_{trs}S$ = 7.8 J K^{-1} mol^{-1}
C_2 phase	
glass transition	T_g = 51 K
phase transition	T_{trs} = 100 K
	$\Delta_{trs}H$ = 80 J mol^{-1}
	$\Delta_{trs}S$ = 0.80 J K^{-1} mol^{-1}
fusion	T_{fus} = 294.29 K,[a] 294.07 K[b] (294.3 K)[c]
	$\Delta_{fus}H$ = 17.07kJ mol^{-1} (19.1 kJ mol^{-1})[c]
	$\Delta_{fus}S$ = 58.0 J K^{-1} mol^{-1} (65 J K^{-1} mol^{-})[c]
liquid	
glass transition	T_g = 218 K (218.7 K)

[a] Pure compound. [b] Calorimetric sample. [c] Reference 17. [d] Not observed.

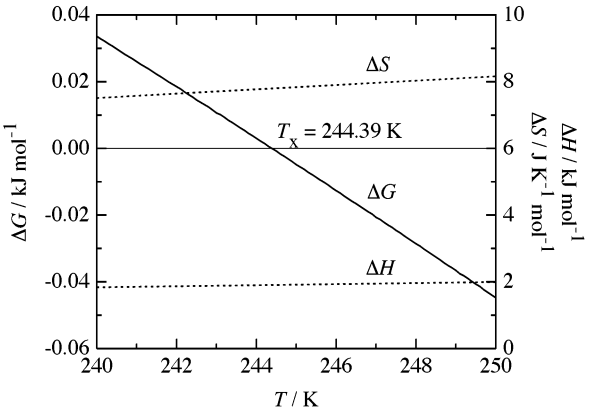

Figure 6. Temperature dependence of the differences in thermodynamic functions (H, S, and G) between the C_2 and C_1 phases. The difference is defined as $\Delta A = A(C_2) - A(C_1)$. At T_x the thermodynamically stable phase changes from the C_1 to C_2 phase upon heating.

The comparison of the Gibbs energy reveals that the thermodynamic stability of two crystalline phases is interchanged at T_x = 244.39 K as shown in Figure 6. One can easily anticipate this Gibbs energy crossover between the C_1 and C_2 phases from the fact that the entropy of fusion for the C_1 phase (67.95 J K^{-1} mol^{-1}) is much larger than that (58.05 J K^{-1} mol^{-1}) for the C_2 phase despite a small difference in their temperature of fusion (294.07 K for the C_2 phase and 287.55 K for the C_1 phase). Although no evidence was detected in the experiments, a phase transition from the C_1 phase to the C_2 phase is, unless kinetically prohibited, expected at this temperature. The enthalpy and the entropy gains expected at this phase transition are calculated as 1.9 kJ mol^{-1} and 7.8 J K^{-1} mol^{-1}, respectively.

The resulting stable phase sequence of c-8*OCB is as follows:

$$C_1 \text{ phase} \xrightarrow{-244.39\text{ K}} C_2 \text{ phase} \xrightarrow{-294.29\text{ K}} \text{liquid}$$

For these stable phases, standard thermodynamic functions obtained in this study are given in Table 2. The inversion of the thermodynamic stability between the C_2 and C_1 phases partly provides a clue to the strange problem found in the previous IR and neutron studies.[17] Namely, the C_2 phase is not the most stable at low temperature. A large vibrational density of states is acceptable for this metastable C_2 phase.

TABLE 2: Standard Thermodynamic Quantities of c-8*OCB for the Stable Phase Sequence

T, K	$C_p°$, J K^{-1} mol^{-1}	$[H°(T) - H°(0)]/T$, J K^{-1} mol^{-1}	$S°(T) - S°(0)$, J K^{-1} mol^{-1}	$-[G°(T) - H°(0)]/T$, J K^{-1} mol^{-1}
		C_1 phase		
10	7.42	2.07	2.78	0.71
20	28.02	9.59	13.83	4.24
30	52.80	19.84	29.84	10.00
40	76.92	31.14	48.38	17.24
50	99.19	42.57	68.00	25.43
60	119.37	53.72	87.90	34.18
70	137.48	64.41	107.68	43.27
80	153.35	74.56	127.10	52.54
90	167.29	84.11	145.99	61.88
100	179.99	93.07	164.28	71.21
110	192.15	101.52	182.00	80.48
120	203.9	109.57	199.23	89.66
130	215.3	117.27	216.0	98.7
140	226.8	124.68	232.4	107.7
150	238.4	131.88	248.4	116.5
160	250.0	138.90	264.2	125.3
170	261.6	145.77	279.7	133.9
180	273.4	152.54	295.0	142.4
190	285.7	159.22	310.1	150.9
200	298.3	165.86	325.1	159.2
210	311.3	172.48	339.9	167.5
220	324.8	179.09	354.7	175.6
230	338.9	185.73	369.5	183.7
240	353.4	192.41	384.2	191.8
244.39	359.6	195.36	390.7	195.3
		C_2 phase		
244.39	375.5	203.2	398.5	195.3
250	383.9	207.1	407.1	200.0
260	399.7	214.2	422.4	208.2
270	417.6	221.4	437.8	216.4
280	438.6	228.8	453.4	224.6
290	463.7	237.4	470.2	232.8
294.29	476.0	242.0	478.4	236.3
		liquid		
294.29	546.6	300.0	536.4	236.3
300	550.0	304.7	546.9	242.2
298.15	548.9	303.2	543.5	240.3

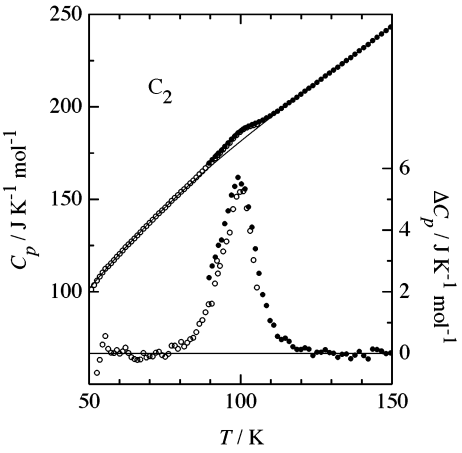

Figure 7. Measured heat capacities and excess heat capacities of c-8*OCB around the phase transition at 100 K. Different symbols distinguish the data obtained in different series of experiments. The solid curve in the upper part is the baseline assumed.

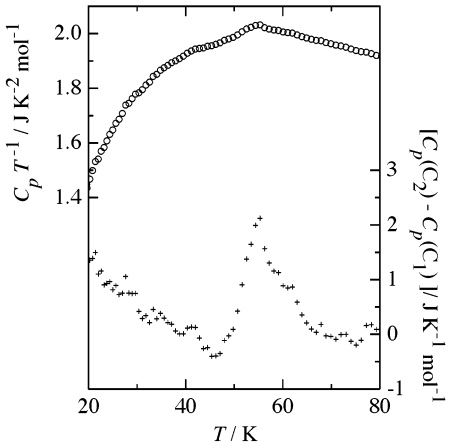

Figure 8. Enclaty (C_p/T) of the C_2 phase (circle) and the difference in heat capacities between the C_2 and C_1 phases (cross) around the glass transition of the C_2 phase.

A very similar example in which the realization of phase transition is extremely difficult despite the Gibbs energy crossover has been reported for a discotic mesogen.[23]

D. Phase Transition and Glass Transition of the c-8*OCB C_2 Phase. As shown in Figure 3, two small anomalies were identified for the C_2 phase, while there was nothing anomalous in the temperature dependence of the heat capacity of the C_1 phase. These two anomalous parts are enlarged in Figures 7 and 8.

Around 100 K, there is a hump in the heat capacity. The anomaly was well-reproduced in repeated runs of measurements. Judging from its shape and magnitude, the anomaly is attributed to a structural phase transition. Assuming a normal heat capacity as a smooth curve, the excess parts were separated as shown in Figure 7. The excess heat capacity gives rise to a maximum at 100 K, which may be regarded as a transition temperature. The integration yields the enthalpy and entropy of transition as 80 J mol^{-1} and 0.8 J K^{-1} mol^{-1}. The smallness of the latter suggests that the phase transition be of the displacive type. Since the structural information is unavailable for the C_2 phase even at room temperature, it is, at present, difficult to discuss further the nature of the phase transition.

Around 50 K an anomaly was detected in the heat capacity as shown in Figure 8. The anomaly is more clearly seen by plotting the difference of the heat capacities of the C_2 and C_1 phases. Besides, the temperature drifts in the equilibration periods showed temperature dependence typical of a glass transition. The anomaly is therefore attributed to a glass transition in the crystalline state. The glass transition temperature T_g is determined as 51 K according to the empirical criterion that at T_g the temperature drift changes its sign from positive to negative in adiabatic heat capacity calorimetry.[6] Now it is clear that below 50 K the phase C_2 is not in the thermodynamic equilibrium due to the prolonged relaxation time of some degrees of freedom: On heating, the frozen-in structural disorder changes into the dynamical one. The magnitude of the step in heat capacity at T_g is about 2 J K^{-1} mol^{-1}. Since a glass transition originates in freezing-in of some disorder, the existence of this glass transition directly proves that there is some residual disorder in the C_2 phase at lower temperatures. The broad IR spectrum and the enhanced vibrational density of states found for the C_2 phase[17] should be attributed to this frozen-in disorder. The degree of disorder, however, is rather small because the residual entropy of the C_2 phase, which was deduced by using the liquid as the common state, is practically zero in comparison with the inaccuracy of the present measurements.

E. Heat Capacities of c-8*OCB. Usually a LQG shows a larger heat capacity than crystalline states due to its loose packing of molecules. This is, however, not the case for c-8*OCB. In the whole temperature range studied, the heat capacity of the C_1 phase is smaller than that of the C_2 phase. For example, as shown in Table 2, the heat capacity of the C_2

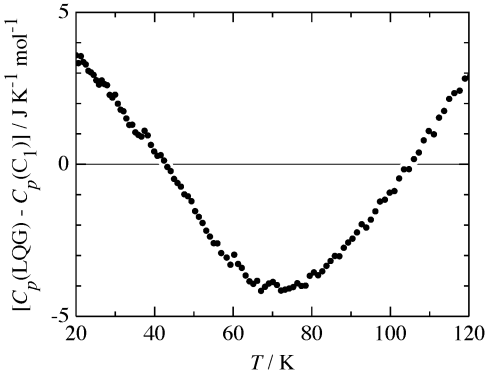

Figure 9. Difference of heat capacities between the LQG and the C_1 phase in the temperature range 20−120 K.

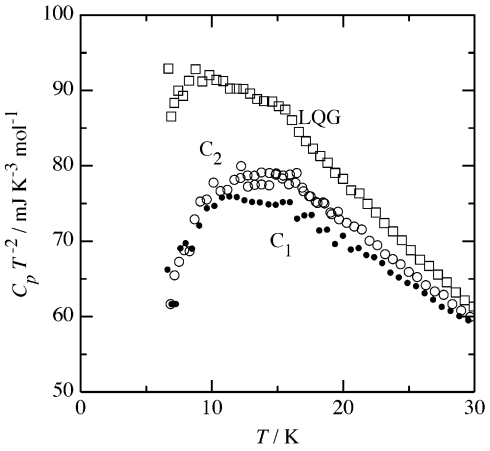

Figure 10. Heat capacities of c-8*OCB at low temperatures: square, LQG; filled circle, C_1 phase; open circle, C_2 phase.

phase at 244.39 K is 15.9 J K^{-1} mol^{-1} larger than that of the C_1 phase. This can be interpreted similarly to the aforementioned case of the relation between LQG and crystals. Above 110 K, the largest heat capacity is observed for the LQG as usual. Between 110 and 40 K, unexpectedly, the heat capacity of the LQG becomes the smallest. This rare observation is presented in Figure 9. Considering the heat capacity of the LQG is smaller than those of two crystalline phases, the cause of this peculiarity seems to be on the LQG side. Structural investigations are necessary to resolve this point.

To compare the calorimetric results of solid forms below 30 K with the neutron spectra[19] (Figure 2), the heat capacities are plotted in Figure 10 in the form of C_pT^{-2} vs. T. One can see that Figures 2 and 10 show the lowest vibrational density of states for the C_1 phase below 20 cm^{-1}. The most disordered form is, needless to say, the LQG for the calorimetry while the neutron result rather suggests that the glassy C_2 phase may be less ordered. Since both the LQG and the C_2 phase are glassy, the actual disorder may depend on details of sample preparation. This discrepancy also may be based on the fact that calorimetry senses an average over all degrees of freedom, while neutron inelastic scattering is sensitive to vibrations involving the hydrogen atoms.

F. Glass Transition of Liquid. Both c-8*OCB and r-8*OCB form LQG on cooling at a moderate rate. They are glass formers. As is evident from Figure 4, their properties are similar. The glass transition temperature is 218 K for c-8*OCB and 217 K for r-8*OCB. Although the following analysis and discussion are made for only one of them, they will apply to the other considering their close similarity.

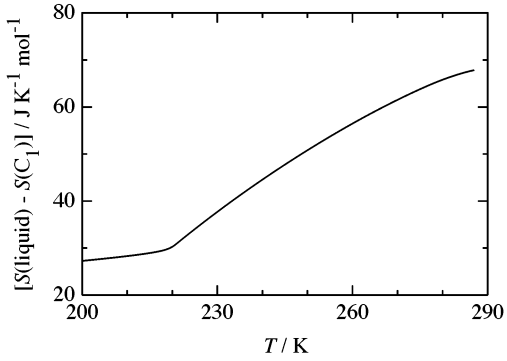

Figure 11. Difference between the calorimetric entropies of the LQG and the C_1 phase.

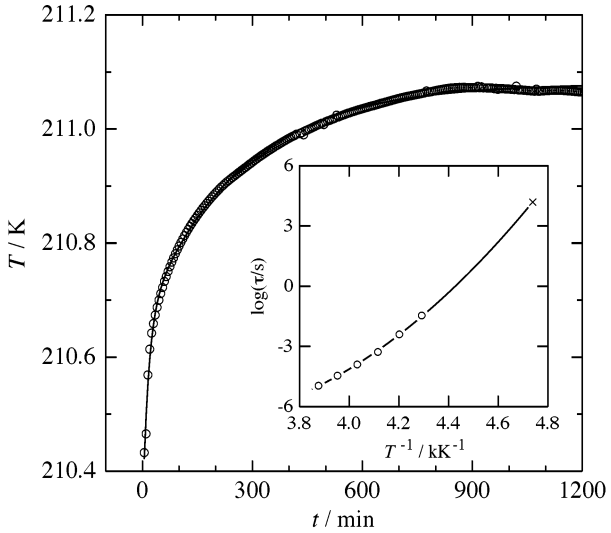

Figure 12. Spontaneous temperature rise due to the enthalpy relaxation around the glass transition for r-8*OCB. The inset shows the temperature dependence of the relaxation times by the dielectric measurements[16] (open circle) and the enthalpy relaxation (cross).

Configurational entropy of LQG is often of interest from the viewpoint of the Adam−Gibbs theory.[24,25] If the difference in vibrational entropy is neglected, the configurational entropy is equal to the difference between the absolute entropies of the LQG and an ordered crystal. This quantity can be calculated for c-8*OCB by using those of the LQG and the C_1 phase and is shown in Figure 11. It is noted that the C_2 phase is not appropriate for this purpose because there are some kinds of disorder as evidenced by the presence of the glass transition around 50 K. By extrapolating the temperature dependence to high temperatures while assuming the functional form $S_c = S_c^{\infty} - AT^{-2}$,[25] the limiting configurational entropy S_c^{∞} is estimated as 124 J K^{-1} mol^{-1}. Although it is hard to assess the validity of neglecting the difference in the vibrational entropy, the size (Z) of the cooperatively rearranging region (CRR) is estimated to be $Z(T_g) \approx 4$ molecules at T_g according to $Z(T) = S_c^{\infty}/S_c(T)$. Similar sizes have been reported for some glass formers.[25]

Since no tendency for crystallization was observed for r-8*OCB, the enthalpy relaxation was safely monitored for a long time. Spontaneous heat evolution was monitored as the record of the temperature under the adiabatic condition around 210 K, where the heat evolution is maximum. The data are presented in Figure 12, in which a small stationary drift (ca. 10^{-4} K min^{-1}) due to incomplete adiabatic control was subtracted. Description of the relaxation by either the simple exponential or the Kohlrausch−Williams−Watts formula[26] was unsuccessful. The good fit was obtained by assuming the sum

of two exponential relaxations

$$T(t) = T_0 + A \exp(-t/\tau_1) + B \exp(-t/\tau_2)$$

The best fit yields $T_0 = 211.08$ K, $A = -0.34$ K, $\tau_1 = 9.3 \times 10^2$ s, $B = -0.42$ K, and $\tau_2 = 1.56 \times 10^4$ s. The success of the fit implies the presence of, at least, two slow relaxation processes. They can be assigned to the short- and long-range correlations in the molecular motion. In the inset of Figure 12 the longer relaxation time is presented together with the dielectric relaxation data.[16] The temperature dependence of the relaxation time is definitely not of the Arrhenius type though a common description by the Vogel−Fulcher−Tammann equation[27,28] typical for glass-forming materials was not successful.

Conclusions

The heat capacities were measured by adiabatic calorimetry down to 6 K on both right-handed isomer and a racemic mixture of 8*OCB. The thermodynamic relationship between two crystalline phases has been established and inversion between stable and metastable crystals has been found for the isomer. The C_2 phase, previously regarded as the stable phase even at low temperature, shows a phase transition of higher order at 100 K and a glass transition in the crystalline state around 50 K. The contradiction between a previous calorimetric study and the results of inelastic neutron scattering and infrared spectroscopy have been resolved as the C_2 phase is at low temperatures not fully ordered and metastable. No crystallization was detected for the racemic mixture.

The behavior around the glass transition has been analyzed. The configurational entropy and corresponding size of the cooperatively rearranging region were estimated for the isomer. Enthalpy relaxation around glass transition seems to have a two-exponential process with a longer relaxation time of 1.5×10^4 s. The temperature dependence of relaxation time from calorimetry and earlier dielectric relaxation data near the glass transition is not of the Arrhenius type. A description by the Vogel−Fulcher−Tammann formula typical for a glass former was not successful.

Acknowledgment. Three of Polish authors (M.M-A., T.W., and J.M.) express their deep gratitude to the Research Center for Molecular Thermodynamics for the invitation, great hospitality, and scientific cooperation during their Visiting Professor Fellowships. The authors acknowledge Professor R. Dabrowski for providing 8*OCB in the isomeric and racemic forms.

References and Notes

(1) Donth, E. *Glass Transition*; Springer-Verlang: Berlin, Germany, 2001.
(2) Palmer, R. G.; Stein, D. L.; Abrahams, E.; Anderson, P. W. *Phys. Rev. Lett.* **1984,** *53*, 958
(3) Cohen, M. H.; Grest, G. S. *Phys. Rev. B* **1981**, *24*, 4091.
(4) Paluch, M.; Ngai, K. L. *J. Chem. Phys.* **2001**, *114*, 10872.
(5) Johari, G. P. *J. Phys. Chem. B* **2003**, *107*, 9063.
(6) Suga, H.; Seki, S. *J. Non-Cryst. Solids* **1974**, *16*, 171.
(7) Leslie-Pelecky, D.; Birge, N. *Phys. Rev. B* **1994**, *50*, 13250.
(8) Sciesinski, J.; Mayer, J.; Wasiutynski, T.; Sciesinska, E.; Wojtowicz, J. *Phase Transitions* **1995**, *54*, 15.
(9) Sorai, M.; Seki, S. *Mol. Cryst. Liq. Cryst.* **1973**, *23*, 299.
(10) Sorai, M.; Saito, K.; Nakamoto, T.; Ikeda, M.; Galyametdinov, Y. G.; Galyametdinova, I.; Eidenschink, R.; Haase, W. *Liq. Cryst.* **2003**, *30*, 861.
(11) Akutsu, H.; Saito, K.; Yamamura, Y.; Kikuchi, K.; Nishikawa, H.; Ikemoto I.; Sorai, M. *J. Phys. Soc. Jpn.* **1999**, *68*, 1968.
(12) Saito, K.; Akutsu, H.; Sorai, M. *Solid State Commun.* **1999**, *111*, 471.
(13) Tozuka, Y.; Yamamura, Y.; Saito, K.; Sorai, M. *J. Chem. Phys.* **2000**, *112*, 2355.
(14) Saito, K.; Okada, M.; Akutsu, H.; Sorai, M. *Chem. Phys. Lett.* **2000**, *318*, 75.
(15) Saito, K.; Kobayashi, H.; Miyazaki, Y.; Sorai, M. *Solid. State Commun.* **2001**, *118*, 611.
(16) Massalska-Arodz, M.; Williams, G.; Thomas, D. K.; Jones, W. J.; Dabrowski, R. *J. Phys. Chem. B* **1999**, *103*, 4197.
(17) Sciesinski, J.; Sciesinska, E.; Massalska-Arodz, M.; Wasiutynski, T.; Zielinski, P. M.; Witko, W. *IEEE Trans. Dielectr. Electr. Insul.* **2001**, *8*, 522.
(18) Sciesinski, J.; Sciesinska, E.; Massalska-Arodz, M. *J. Mol. Struct.* **2001**, *596*, 229.
(19) Mayer, J.; Krawczyk, J.; Janik, J. A.; Massalska-Arodz, M.; Natkaniec, I.; Steinsvoll, O. *Physica B*. Submitted for publication.
(20) Brucket, T.; Urban, S.; Wurflinger, A. *Ber. Bunsen-Ges. Phys. Chem.* **1996**, *100*, 1133.
(21) Yamamura, Y.; Saito, K.; Saitoh, H.; Matsuyama, H.; Kikuchi, K.; Ikemoto, I. *J. Phys. Chem. Solids* **1995**, *56*, 107.
(22) Angell, C. A.; Smith, D. L. *J. Phys. Chem.* **1982**, *86*, 3845.
(23) Van Hecke, G. R.; Kaji, K.; Sorai, M. *Mol. Cryst. Liq. Cryst.* **1986**, *136*, 197.
(24) Adam, G.; Gibbs, J. H. *J. Chem. Phys.* **1965**, *43*, 139.
(25) Yamamuro, O.; Tsukushi, I.; Lindquvist, A.; Takahara, S.; Ishikawa, M.; Matsuo, T. *J. Phys. Chem. B* **1998**, *102*, 1605.
(26) Williams, G.; Watts, D. C. *Trans. Faraday Soc.* **1970**, *66*, 80.
(27) Vogel, H. *Phys. Z.* **1921**, *22*, 645.
(28) Fulcher, S. G. *J. Am. Ceram. Soc.* **1923**, *8*, 339.